Ion Accumulation in a Biological Calcium Channel: Effects of Solvent and Confining Pressure

Wolfgang Nonner* and Dirk Gillespie[†]

Department of Physiology and Biophysics, University of Miami School of Medicine, Miami, Florida 33101

Douglas Henderson[‡]

Department of Chemistry and Biochemistry, Brigham Young University, Provo, Utah 84602

Bob Eisenberg[§]

Department of Molecular Biophysics and Physiology, Rush Medical College, Chicago, Illinois 60612

Biological L-type calcium channels selectively accumulate Ca^{2+}, even when there is 10^5 more Na^+ in the surrounding electrolyte solution. Like other Ca^{2+}-chelating molecules, the L-type calcium channel has four carboxylate groups that contain eight oxygen ions. In this modeling study, these oxygens are confined to a small subvolume of the channel protein (the "filter") that is embedded in a bulk electrolyte solution (the "bath"). With the system in equilibrium, the concentrations of the ions and water in the filter are computed, given their concentrations in the bath. The excess thermodynamic properties are calculated using the mean spherical approximation (MSA), with water modeled as an uncharged hard sphere [the so-called solvent primitive model (SPM)] and a dielectric coefficient. Use of the SPM is an extension of previous work, where water was modeled as an amorphous dielectric. Other new aspects included in this study are changing the volume of the filter in response to the pressure generated by the water and ions in the filter and modeling solvation effects in more detail. The model is calibrated with a single experimental measurement. Predictions are compared to experimental results, where available, and future experiments are suggested. Finally, the model is considered as a Ca^{2+} signal transducer able to perform substantial mechanical work in a Ca^{2+} regulated protein.

1. Introduction

Living cells use transient increases of intracellular Ca^{2+} concentration to control many proteins, including, for example, those that make the heart beat.[1] As transmembrane proteins, Ca channels provide a specific ionic pathway that allows extracellular Ca^{2+} ions to flow into the cell for use in intracellular signaling. Most proteins that are sensitive to Ca^{2+} accumulate the ion in specific binding sites involving several carboxylate groups of glutamate or aspartate residues. The L-type Ca channel considered here is an example; its aqueous pore binds calcium ions in a ring of four glutamate residues called the EEEE locus.[2−9]

Two recent papers have addressed the question of how such a locus might accumulate Ca^{2+} from environments that contain a large background concentration of other ions. Each paper modeled the locus as an ensemble of eight half-charged oxygen ions (representing four carboxylate groups) confined to a small volume. Nonner, Catacuzzeno, and Eisenberg (NCE)[10] described the electrolyte confined in this "selectivity filter" as an isotropic solution using the mean spherical approximation (MSA). Boda, Busath, Henderson, and Sokołowski (BBHS)[11,12] described the electrolyte using Monte Carlo simulations in which the filter

was represented as an infinite cylinder bounded by a hard wall and ions were represented as charged, hard spheres. Both studies used the primitive model (PM) of electrolyte solutions, in which water is a continuous dielectric. Both papers showed that such a system accumulates Ca^{2+} over Na^+ and Cl^- from a bath containing micromolar $CaCl_2$ and 0.1 M NaCl. Ca^{2+} provides the same mobile charge as two Na^+, but in half the volume, that is, the calciums are less crowded in this system than the sodiums and they provide better screening.

This paper extends the NCE and BBHS models of the EEEE locus in several ways. First, water is included in the model as a hard-sphere fluid, the so-called solvent primitive model (SPM) of ionic solutions. The SPM is more successful than the PM in studies of solvation forces[13] and simulations of the electrical double layer.[14,15] Furthermore, Goulding et al.[16,17] have demonstrated "entropic selectivity in microporous materials" arising solely from hard-sphere interactions of uncharged solutes and solvent.

The second extension of previous work allows the solvents of the bath and filter to be distinguished. Changes of solvation energy associated with the transition of ions from the bath to the filter are estimated using experimental hydration energies, which are specific to each ion species. This allows solvation effects (through the dielectric coefficient of the filter) to be treated in more detail.
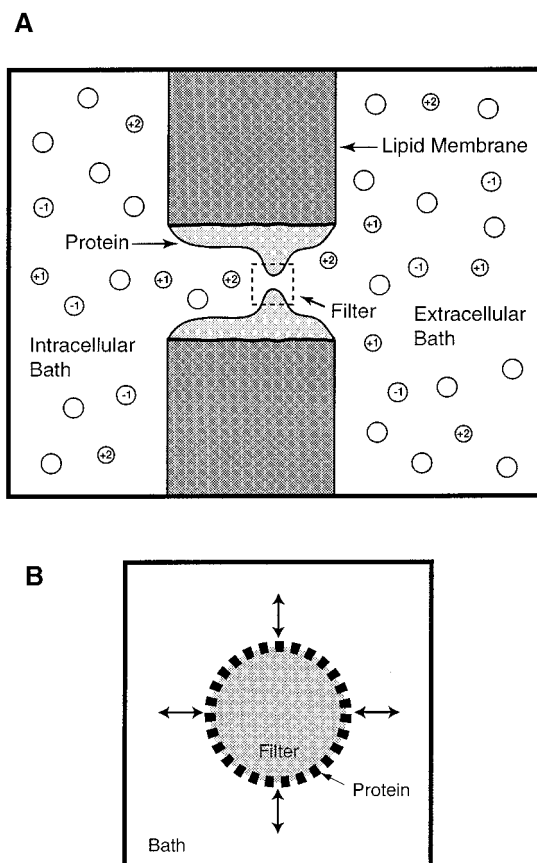
The third change relaxes the previous assumption that the volume of the selectivity filter is constant. Instead, the filter

---

* Corresponding author. Fax: (305) 243-5931. E-mail: wnonner@chroma.med.miami.edu.
† Fax: (305) 243-5931. E-mail: dirkg@chroma.med.miami.edu.
‡ Fax: (801) 378-5474. E-mail: doug@huey.byu.edu.
§ Fax: (312) 942-8711. E-mail: beisenbe@rush.edu.

A

B

Figure 1. In panel A is shown a representation of a typical channel embedded in a lipid membrane that separates two baths of known ionic concentrations. In a typical experiment to measure current/voltage relations, an electrostatic potential is applied across the membrane. When the baths have identical composition and no potential is applied, there is equilibrium (i.e., no net current flow from any species). This is the situation examined in this paper with the highly idealized selectivity filter shown in panel B. Because the two baths are identical, they are merged into one. Furthermore, the solution inside the filter (shaded area in panel B) is treated as a bulk, homogeneous fluid that contains a density of negatively charged groups that represent the four carboxylates present in the selectivity filter of a Ca channel (see the main text). The purpose of the protein in this idealized situation is to exert a confining pressure on the filter. The arrows in panel B indicate that the volume of the filter is variable (i.e., the protein is flexible) depending on the pressure exerted by the contents of the filter.

volume is allowed to change as the pressure in the filter changes. A variable filter volume not only prevents forces inside the channel from becoming so large that they would break strong noncovalent bonds in other systems[18,19] but also has substantial effects on ion accumulation. Furthermore, such mechanical effects of Ca^{2+} accumulation seem strong enough to drive conformation changes of calcium-binding proteins.

2. Model of the Filter/Bath System

Figure 1A shows a scheme representing the ion-selective pore of the Ca channel ("filter" for short) and its environment. In a real Ca channel, this filter is a short axial subsection of a transmembrane pore whose wall is formed by the channel protein. The real filter thus communicates with two electrolyte reservoirs, the intra- and the extracellular solutions. For our analysis of equilibrium ion accumulation, we represent the two electrolyte reservoirs (of necessarily equal compositions) as a single large reservoir that surrounds the filter (Figure 1B). The protein is reduced to a semipermeable boundary around the filter

(see below), which also provides a mechanical enclosure such that different pressures can be maintained in the filter and reservoir compartments.

Ions and water can diffuse between filter and bath. The filter also contains four carboxylate groups that extend from glutamate side chains into the pore of the Ca channel (EEEE locus) and thus are tethered to the pore wall formed by the protein. They are the fixed charge in traditional models of ion exchangers. These four carboxylates are represented as eight half-charged oxygen ions in our model. The role of the tethers is idealized: they confine the oxygens to a volume (thus defining a filter compartment) but allow them to move in an unrestricted manner within the compartment while coordinating with exchangeable species that enter from the bath. In Figure 1B this effect of the tethers is represented by the semipermeable boundary that surrounds the filter (dashed line) and allows water and mobile (but not oxygen) ions to be exchanged with the bath.

Within the filter of our model, exchangeable molecules (such as counterions and water) compete for space with the carboxylate oxygens and other atoms of the protein that dwell in the vicinity of the oxygen ions. The contents of the filter are described as a concentrated electrolyte solution in a volume determined by the bounding array of protein atoms. The protein can advance or retreat, depending on the pressure created by the filter contents and the force field provided by the protein. We model this protein force field as a confining pressure that the protein exerts on the contents of the filter.

Filter and bath electrolytes are described as two homogeneous bulk solutions that communicate as described above, and the channel protein confines the contents of the filter by the pressure it exerts. In this way we allow the mechanical and excluded-volume interactions to extend beyond the filter volume into the protein, so there is no rigid, smooth boundary between the channel protein and the contents of the channel. Instead, mechanical and entropic interactions of the filter contents with the wall are described by the confining pressure that is exerted by the protein. Note that because we model both the bath and the filter as bulk solutions, our notion of "filter volume" does not assume a particular geometric shape of the filter space and that the confining pressure of the protein in this model is balanced by the pressure of the homogeneous solution in the filter.

Our computations ignore anisotropy that is necessarily present at the interfaces between the filter, protein, and bath. However, the electrostatic anisotropy likely has relatively small significance for the screening in the filter, because the screening radius computed for the filter is less than 0.1 nm, substantially smaller than the dimensions of the filter. Indeed, previous work comparing bulk analysis with a "nanoscale" Poisson−Nernst−Planck description of the Ca channel,[20] as well as the simulations of BBHS, indicate that describing the filter as an electroneutral bulk solution is quite reasonable for exploring mechanisms involved in the ionic selectivity of such biological channels.

Last, it is important to note that, as in NCE, the present model does not include the possibility that carboxylate ions of the Ca channel are protonated. Thus, our computations apply to bath concentrations of hydrogen ion that do not result in "proton block" of the channel (pH >9).

2.1. Thermodynamics. The filter solution is described as an ensemble that exchanges material and heat with a large reservoir where temperature and chemical potentials are constant. Since we will simulate situations in which either a fixed volume or a fixed pressure is imposed on the filter ensemble, we derive the thermodynamics for any pressure/volume closure. The only

situation-specific reference we make is that the external pressure comes from the protein surrounding the channel (P_{prot}). The thermodynamic potential generally describing this system is the availability, A:[21]

$$A = E - TS + P_{prot}V - \sum_i \mu_{B,i}N_i \qquad (1)$$

where variables with (first) subscript "B" apply to the bath, variables with subscript "prot" to the protein, and variables not subscripted to the filter. E is the internal energy, T the temperature, S the entropy, P the pressure, V the volume, $\mu_{B,i}$ the chemical potential of species i in the bath, and N_i the number of molecules of that species in the filter.

Following an earlier analysis of the Ca channel,[20] we treat the contents of the filter as an electroneutral bulk solution. Furthermore, treating the contents of the filter as a bulk solution described by the MSA requires electroneutrality. (However, it is interesting to note studies of confined electrolytes[11,12] show that the confined fluid need not be exactly electroneutral.) Thus,

$$e_0 \sum_j z_j N_j = 0 \qquad (2)$$

The index j denotes *any* species in the filter (including all exchangeable particles and particles confined to the filter), while the index i introduced in eq 1 refers exclusively to the exchangeable particles. z_j is the valence of species j and e_0 the proton charge. Subject to this constraint, we seek to minimize the availability with respect to the number of molecules of all exchangeable species in the filter and the filter volume.

Using the thermodynamic relation

$$G = E - TS + P_{prot}V = \sum_j \mu_j N_j \qquad (3)$$

for the Gibbs energy G[21] and the Gibbs−Duhem relation, we find that A is minimized with respect to the number of molecules of mobile species i when the chemical potentials of the species in the filter and bath are equal:

$$\mu_i = \mu_i^0 + \mu_i^{ex} + kT \ln \rho_i + e_0 z_i \Psi = \mu_{B,i} =$$
$$\mu_{B,i}^0 + \mu_{B,i}^{ex} + kT \ln \rho_{B,i} \quad (4)$$

where μ_i^{ex} is the excess chemical potential of mobile species i associated with the electrostatic and excluded-volume interactions in the filter, μ_i^0 the standard chemical potential (describing solvation), ρ_i the number density of species i ($\rho_i = N_i/V$), and Ψ the electrical potential of the filter relative to the bath (Donnan potential). k is the Boltzmann constant.

Using the thermodynamic relation (at constant temperature and N_i)

$$\frac{\partial(E - TS)}{\partial V} = -P \qquad (5)$$

and assuming (see below) that P_{prot} is constant (i.e., independent of filter volume), we find that A is minimal with respect to filter volume when the pressures in the filter and protein are balanced:

$$P = P_{prot} \qquad (6)$$

No description (i.e., "closure") for $P_{prot}(V)$ in the Ca channel is known, as far as we are aware. In section 3.2 we will consider the case of constant pressure that could result simply if the protein were much larger than the filter space or if the filter

were a cylinder that could expand/shrink only in the radial dimension with an elastic force f proportional to the circumference of that cylinder. Then $f \propto R$ and the protein exerts the pressure

$$P_{prot} = f/(2RL) \propto 1/(2L) = const \qquad (7)$$

where R and L are the radius and length of the cylinder.

Note that the minimal availability is not zero, as it would be if all species, including carboxylate oxygens, were to equilibrate between the filter and the bath; confining the carboxylates to one region makes the minimal availability a finite number that represents the energetic cost of the confinement. Substitution of eq 3 into eq 1 shows that, at the minimum determined under this condition, the terms associated with the mobile ion species cancel, because the chemical potentials of these species are the same in both locations. Thus, the availability is given by the Gibbs energy of the oxygen ions

$$A(N_j,V) = N_{Ox}\mu_{Ox}(N_j,V) \qquad (8)$$

which summarizes the energetics in the EEEE locus that underlie the accumulation of mobile ions from baths of varied composition.

2.2. Excess Thermodynamic Properties. All thermodynamic properties of the filter and bath solutions were expressed as sums of ideal and excess contributions and calculated from statistical mechanics. We computed the excess thermodynamic properties with the MSA theory of bulk electrolytes,[22−29] in which ions are described as charged, hard spheres. Ionic excess chemical potentials in the bath were computed with the PM of water as a continuum dielectric, while ionic excess chemical potentials and pressure in the filter were computed with the SPM of water. In the SPM, water molecules are described as a species of uncharged, hard spheres; dielectric properties of the solvent and solution are represented by a continuum dielectric as they are in the PM.

For the bath solution, we computed ionic excess chemical potentials with respect to the infinitely dilute solution in water, using the PM/MSA description of bulk electrolytes developed by Simonin et al.[28,29] The standard and excess chemical potentials of water in the bath were set to zero. Any theory that gives the chemical potentials of ions and solvent accurately ($\mu_{B,i}$ in eq 4) can be used to describe the bulk solution, since these are the only properties of the bath electrolyte we use. Because the PM/MSA describes these aspects of bulk solution well, we chose this model.

In the filter we used the SPM/MSA model of electrolyte solutions, where the solvent was assigned the hard-sphere diameter of water and the dielectric aspect of the solvent/protein was described by a dielectric coefficient that was significantly lower than that of pure bulk water. This coefficient parametrizes the local polarization produced by the electrolytes in the filter. The dielectric coefficient was assigned a fixed value, independent of the composition of the filter electrolyte.

Because the filter and bath solvents were not identical, the transfer of an ion of species i between the filter and bath solutions involved a change in standard chemical potentials. For the standard chemical potentials in the bath we used experimental bulk molar Gibbs energies of hydration, while standard chemical potentials in the filter were estimated by scaling bulk hydration energies in inverse proportion to the dielectric coefficients, following the Born treatment of hydration.[30] The resulting change in standard chemical potential in going from

the bath to the filter was

$$\Delta\mu_i^0 = \mu_i^0 - \mu_{B,i}^0 = \mu_{w,i}^0 \frac{\epsilon - \epsilon_w}{\epsilon(\epsilon_w - 1)} \tag{9}$$

where ϵ is the dielectric coefficient of the filter solvent and ϵ_w that of pure water, and $\mu_{w,i}^0$ is the molar Gibbs energy of solvation in water. The standard chemical potentials of water in filter and bath were set equal, so $\Delta\mu_w^0 = 0$.

In the filter solution, the excess chemical potential of a species i (ion or water) is expressed in the components

$$\mu_i^{ex} = \mu_i^{ES} + \mu_i^{HS} \tag{10}$$

The electrostatic (ES) component is described by

$$\mu_i^{ES} = -\frac{e_0^2}{4\pi\epsilon\epsilon_0}\left[\frac{\Gamma z_i^2}{1 + \Gamma\sigma_i} + \eta\sigma_i\left(\frac{2z_i - \eta\sigma_i^2}{1 + \Gamma\sigma_i} + \frac{\eta\sigma_i^2}{3}\right)\right] \tag{11}$$

where ϵ_0 is the permittivity of a vacuum. The MSA screening parameter Γ is given by the implicit relation

$$4\Gamma^2 = \frac{e_0^2}{kT\epsilon\epsilon_0}\sum_i \rho_i\left[\frac{z_i - \eta\sigma_i^2}{1 + \Gamma\sigma_i}\right]^2 \tag{12}$$

and the MSA parameter η represents the effects of nonuniform molecular diameters σ_i:

$$\eta = \frac{1}{\Omega}\frac{\pi}{2\Delta}\sum_j \frac{\rho_j\sigma_j z_j}{1 + \Gamma\sigma_j} \tag{13}$$

$$\Omega = 1 + \frac{\pi}{2\Delta}\sum_j \frac{\rho_j\sigma_j^3}{1 + \Gamma\sigma_j} \tag{14}$$

where Δ is defined below. The electrostatic interactions contribute the (negative) excess pressure

$$P^{ES} = -\frac{\Gamma^3}{3\pi} - \frac{e_0^2\eta^2}{2\pi^2 kT\epsilon\epsilon_0} \tag{15}$$

The hard-sphere (HS) component of the excess chemical potential, expressed relative to the pure filter solvent, is

$$\mu_i^{HS} = \mu_{act,i}^{HS} - \mu_{ref,i}^{HS} \tag{16}$$

where the terms on the right-hand side are computed from the expressions[31,32]

$$\frac{\mu_{x,i}^{HS}}{kT} = -\ln\Delta + \frac{3\xi_2\sigma_i + 3\xi_1\sigma_i^2}{\Delta} + \frac{9\xi_2^2\sigma_i^2}{2\Delta^2} + \frac{\pi P_x^{HS}\sigma_i^3}{6kT} \tag{17}$$

$$\frac{\pi P_x^{HS}}{6kT} = \frac{\xi_0}{\Delta} + \frac{3\xi_1\xi_2}{\Delta^2} + \frac{3\xi_2^3}{\Delta^3} \tag{18}$$

$$\xi_n = \frac{\pi}{6}\sum_j \rho_{x,j}\sigma_j^n \tag{19}$$

$$\Delta = 1 - \xi_3 \tag{20}$$

TABLE 1: Molecular Parameters[a]

species	σ (nm)	CN	μ_w^0 (kJ mol^{-1})	species	σ (nm)	CN	μ_w^0 (kJ mol^{-1})
Li$^+$	0.133	5	−529.4	Ca^{2+}	0.214	7	−1608.3
Na$^+$	0.200	5	−423.7	Ba^{2+}	0.278	7	−1351.7
K$^+$	0.276	6	−351.9	Cl$^-$	0.362	6	−304.0
Cs$^+$	0.340	6	−306.1	O$^{1/2-}$	0.280	6	−
Mg^{2+}	0.178	8	−1931.4	H$_2$O	0.280	−	−

[a] Ionic diameters σ were taken from Shannon and Prewitt[39] and hydration energies μ_w^0 from Fawcett.[49] CN is the coordination number. The diameter for Li$^+$ is the mean of the coordination 4 and 6 diameters.

For the ions, the actual densities (subscript "act") are the densities in the filter solution and the reference densities (subscript "ref") are zero (infinitely dilute solution of the ion species in filter solvent). For the solvent (neutral, hard spheres with the diameter of water), the actual density is that of the solvent present in the filter and the reference density is that of pure water. The subtraction in eq 16 establishes (at infinite dilution) the filter solvent as the reference for excess chemical potentials in the filter. Similarly, the (excess plus ideal) pressure in the hard-sphere liquid of the filter is computed from

$$P^{HS} = P_{act}^{HS} - P_{ref}^{HS} \tag{21}$$

Solvent and ionic diameters used to model the filter solution are listed in Table 1, together with the ionic hydration energies used in eq 9.

2.3. Numerical Methods. The numerical problem was to find the densities of the mobile ions in the filter, the voltage, and the volume of the filter that simultaneously satisfy eqs 2, 4, and 6 and thus minimize the availability (eq 1). Given were the densities in the bath ($\rho_{B,i}$), the (constant) mechanical pressure exerted by the protein (P_{prot}), and the dielectric coefficient of the filter solvent (ϵ).

For a fixed and given volume V, the excess chemical potentials μ_i^{ex} of the ions in the filter were calculated by iteration. The initialization (the zeroeth step of the iteration) was done as follows:

(1) Compute the excess chemical potentials in the bath $\mu_{B,i}^{ex}$ from the given ionic densities $\rho_{B,i}$. For water, set the terms μ_i^0, $\mu_{B,i}^0$, and $\mu_{B,i}^{ex}$ to zero, so that the distribution of water in the model is determined only by the ideal and hard-sphere interactions.

(2) Compute the solvation energies of the ions in the filter from eq 9 using the given ϵ and the hydration energies listed in Table 1.

(3) Set the initial guesses for the excess chemical potentials of the ions in the filter and the voltage: $\mu_i^{ex}(0) = 0$ and $\Psi(0) = 0$.

After m steps of the iteration, the following algorithm was used for iteration step $m + 1$:

(1) Compute the densities of the mobile ions and water in the filter $\rho_i(m+1)$ from eq 4 using $\mu_i^{ex}(m)$ and $\Psi(m)$, the values from the previous iteration step.

(2) Solve the MSA equations (eqs 10−20) for the excess chemical potentials in the filter μ_i^{ex} and the pressure $P(m + 1)$ using the current values of $\rho_i(m + 1)$. In these equations the MSA screening parameter Γ was determined using Brent's algorithm for finding the root of a one-dimensional algebraic equation.[33]

Ion Accumulation in a Biological Ca Channel

J. Phys. Chem. B, Vol. 105, No. 27, 2001 **6431**

(3) Attenuate the computed values μ_i^{ex} with the values from the previous iteration step by

$$\mu_i^{ex}(m + 1) = \frac{\alpha \mu_i^{ex}(m) + \mu_i^{ex}}{\alpha + 1} \quad (22)$$

where the factor α ranges between 2 and 20. This is necessary for the iteration to converge.

(4) Find the voltage $\Psi(m + 1)$ by (a) solving eq 4 for ρ_i as a function of the Ψ using the current value of $\mu_i^{ex}(m + 1)$ and (b) substituting this into eq 2 to get an algebraic equation for $\Psi(m + 1)$ that is solved numerically with Brent's method.

If $e_0|\Psi(m + 1) - \Psi(m)|/(kT) > 10^{-8}$, then the iteration is done again. Otherwise the iteration is stopped.

At the end of the iteration the excess chemical potentials of the ions in the filter μ_i^{ex} and the pressure P have been calculated for a given volume V. The resulting relation of P as a function of V can then be used to determine the volume at which the pressure from the ions in the filter balances the pressure from the protein (cf. eq 6). Specifically, the equation

$$P(V) - P_{prot} = 0 \quad (23)$$

is solved by Brent's method.

3. Results and Discussion

The model of the EEEE locus discussed here involves a particulate model of water (SPM) and a fixed number of oxygen ions that are confined in a variable volume. In the earlier models of NCE and BBHS, water was modeled as an amorphous dielectric (PM), and oxygen ions were confined in a fixed volume. It is expected that variation of volume and the resulting variation in the density of oxygen ions will change the affinities of the filter for solutes and solvent. Altered affinities will result in altered densities of exchangeable solutes and solvent and thus change the volume of the filter. The equations describing the system must be solved self-consistently, including an equation relating pressure to volume. Before introducing a closure that relates pressure in the filter to volume, we consider properties of the filter as computed for a range of assumed volumes.

Figure 2A shows computed numbers of Ca^{2+}, Na^+, and water molecules that partition from the bath into the filter. These numbers are the product of the computed particle densities and the filter volume. The aqueous bath solution contains 0.1 M NaCl and 1 μM $CaCl_2$. Experiments suggest that in this situation the channel contains equivalent amounts of Ca^{2+} and Na^+ (see below); we will refer to this as "physiological selectivity". In this figure, the filter contains eight half-charged oxygen ions in a volume that is stepped from 0.6 to $\approx$0.2 nm^3. The dielectric coefficient in the filter is 10. The filter accumulates Ca^{2+} from the bath when the oxygen ions become concentrated in a volume less than 0.4 nm^3. Equivalent charges of Ca^{2+} and Na^+ are accumulated, and thus physiological selectivity occurs, if the volume is $\approx$0.25 nm^3. In this calculation, selectivity is found in a filter volume substantially smaller than that used by NCE[10] (0.375 nm^3). The small volume is populated by the oxygen ions and their counterions. Water is virtually excluded.

Figure 2B plots pressures in the filter that correspond to the computations of Figure 2A. Shown are the (ideal and excess) pressure due to all the hard spheres in the filter (HS), the excess pressure due to electrostatic ion–ion interaction (ES), and their sum. Substantial negative pressures (describing attractive forces) arise from the Coulombic interactions among the ions, but this pressure is more than compensated by the positive pressures
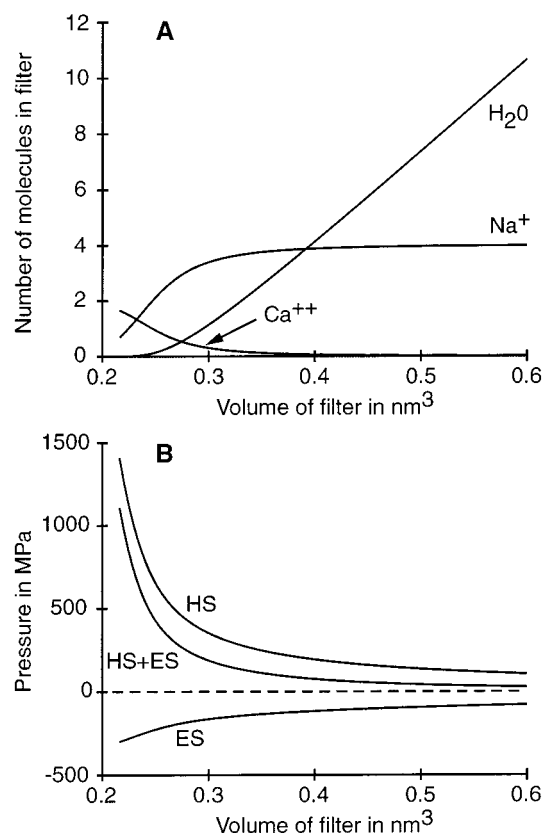

Figure 2. Number of mobile particles (A) and pressures (B) in the filter of the model. HS, ideal plus excluded volume pressure; ES, cohesive pressure due to electrostatic ion–ion interaction. In these computations, the filter was assigned the varied volume shown on the abscissa and a fixed dielectric coefficient of 10. The bath contained 0.1 M NaCl and 10^{-6} M $CaCl_2$. The number of accumulated Cl^- is so small that it could not be distinguished from the baseline in panel A.

(describing repulsive forces) arising from the high density of hard spheres; a net positive pressure is found. Thus, external pressure ($\approx$400 MPa) is needed to maintain the volume of the filter in which physiological selectivity occurs. Note that the only cohesive force explicitly included in this model is Coulombic ion–ion interaction; all other cohesive forces are part of the effective pressure exerted by the protein to confine the oxygen ions.

At a pressure of 400 MPa, the packing fraction of particles ($\pi\Sigma_i\rho_i\sigma_i^3/6$) is larger in the modeled EEEE locus than it is in the bath (e.g., between 0.418 and 0.440 in the computations of Figure 4, compared to 0.384 for the bath). Water thus experiences significantly less excluded-volume repulsion in the bath than it does in the filter.

The SPM-based computations of Figure 2 predict physiological selectivity in a smaller volume than that previously estimated using the PM. This can be traced to the different descriptions of the solvent in the PM and SPM. The different estimates of volume indicate that the two models are not equivalent in describing one significant role that the solvent plays in ionic selectivity. Specifically, if we describe the filter and bath solutions in the PM, packing fractions of particles are computed from the volume demands made by the ions, but not from those made by the solvent. Since ionic densities in the two compartments differ substantially, the PM computes strongly asymmetric pressures due to excluded volume. In reality (and in the SPM), such a large pressure difference does not arise. With the solvent included as a particulate species, packing fractions in both
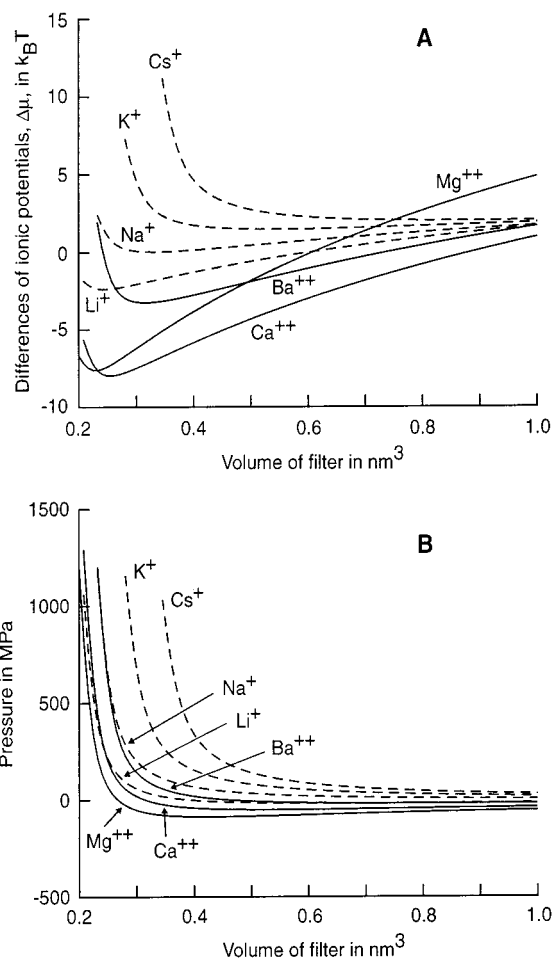
Figure 3. Differences of combined standard and excess chemical potentials of ions in the filter and bath (A) and associated total pressures (B). A separate computation was done for each ion in which the filter volume was varied over the range shown on the abscissa. The bath contained 0.1 M of the chloride salt of the tested ion. The results for monovalent cations are represented as dashed lines for clarity. At filter volumes much larger than shown here, the potential differences approach the differences of solvation energies, $\mu_i^0 - \mu_{B,i}^0$; these are (in kT): 18.9 (Li$^+$), 15.1 (Na$^+$), 12.5 (K$^+$), 10.9 (Cs$^+$), 68.9 (Mg^{2+}), 57.3 (Ca^{2+}), and 48.2 (Ba^{2+}). Some pressure/volume curves in panel B involve a region of negative compressibility, which is due to electrostriction.

compartments are more balanced and so are the effects of excluded volume.

The calculations also suggest that the pressure required for water extrusion is much less than the pressure needed to include additional entering ions into an already densely packed filter. If the filter volume is large enough to admit several water molecules, volume demands made by entering mobile ions are satisfied by removing water from the filter. It is not until the filter volume decreases to the point that water is almost completely extruded from the filter that the excluded volume becomes significant for ionic selectivity. The mobile ions entering the filter then compete for space with the tethered particles always present in the filter, as is revealed by the substantial pressure changes that occur in the filter (Figure 2B). If the filter is to distinguish between the volumes excluded by different species of mobile ions, the filter must not contain substantial amounts of mobile solvent.

If physiological selectivity arises in a very small volume, one expects that accumulation of ions of different diameters occurs with distinct selectivities. All alkali and several alkali earth ions

permeate L-type Ca channels.[34] Selectivities with respect to different ion species i can be assessed using the difference of the combined standard and excess chemical potentials between filter and bath:

$$\Delta\mu_i = \mu_i^0 + \mu_i^{ex} - (\mu_{B,i}^0 + \mu_{B,i}^{ex}) \qquad (24)$$

This represents the ionic affinity due to the local interactions in the filter (excluding the effect of the Donnan potential Ψ). Figure 3 shows $\Delta\mu_i$ computed for a range of filter volumes (panel A), as well the corresponding pressures in the filter (panel B). At volumes much larger than those included in Figure 3A, $\Delta\mu_i$ approaches $\mu_i^0 - \mu_{B,i}^0$, the molar Gibbs energy of transferring the ion from the bath solvent to the solvent in the filter; values for this energy are listed in the legend of Figure 3. As the volume of the filter is reduced, $\Delta\mu_i$ first becomes smaller (and even becomes significantly negative with some ions), but eventually rises steeply. The reduction in $\Delta\mu_i$ is produced by the electrostatic ion–ion interactions that become stronger as oxygen ions and counterions are concentrated in the filter. The steep rise in selectivity seen at very small volumes is produced by crowding, i.e., the mutual volume exclusion among these ions.

3.1. External Parameters. *Filter Volume and Pressure*. If the filter volume were fixed at a volume in which physiological Ca^{2+}/Na$^+$ selectivity occurs (≈ 0.25 nm^3), accumulation of the larger alkali ions would result in pressures (Figure 3B) too large to be balanced by the noncovalent forces that stabilize the native structure of the channel protein. For example, a pressure of 400 MPa acting in a cylindrical filter 0.5 nm in length and 1 nm in diameter (volume ≈ 0.39 nm^3) would strain the wall of the filter with a force of 200 pN. This is a large force when compared to the mechanical forces in other protein systems with a strong noncovalent protein–ligand interaction. For example, the complex of streptavidin and biotin is broken by forces of ≈ 260 pN,[18] and transmembrane loops of bacteriorhodopsin (a very stable membrane protein) are pulled out of the native structure by forces of 100–200 pN.[19] For that reason, we do not believe that the selectivity filter can maintain pressures much larger than 400 MPa.

It also seems unlikely that the confining pressure is much smaller than 100 MPa. In that case, our computations predict very large expansions of the filter when only counterions of large diameter are available (Figure 3B). In simulations of ion binding described below, we assume a constant confining pressure of 400 MPa. The actual pressure required from the protein would be diminished by any cohesive pressures that exist but are not explicitly in the model of the filter.

It is interesting to compare theoretically estimated filter volumes with filter dimensions inferred from experimental work. If we assume that a carboxylate group spans an axial length of ≈ 0.5 nm and take this as the axial dimension of the filter, a cylindrical filter of volume 0.25–0.4 nm^3 (see Figure 5B) would have a diameter between 0.8 and 1 nm. It is important to note, however, that the filter volume we describe is a sample from a bulk solution whose virtual boundary is generally overlapped by particles from both sides (e.g., there is no hard wall). The size of the oxygen-free cross section of such a filter is consistent with the current view that the Ca channel has an effective diameter ≈ 0.6 nm,[35] which is substantially larger than that of Ca^{2+}.

Electrical Polarization in the Filter. In our model, ions moving from the bath to the filter experience a change in solvation energy as they enter a solvent of low dielectric

Ion Accumulation in a Biological Ca Channel

J. Phys. Chem. B, Vol. 105, No. 27, 2001 **6433**
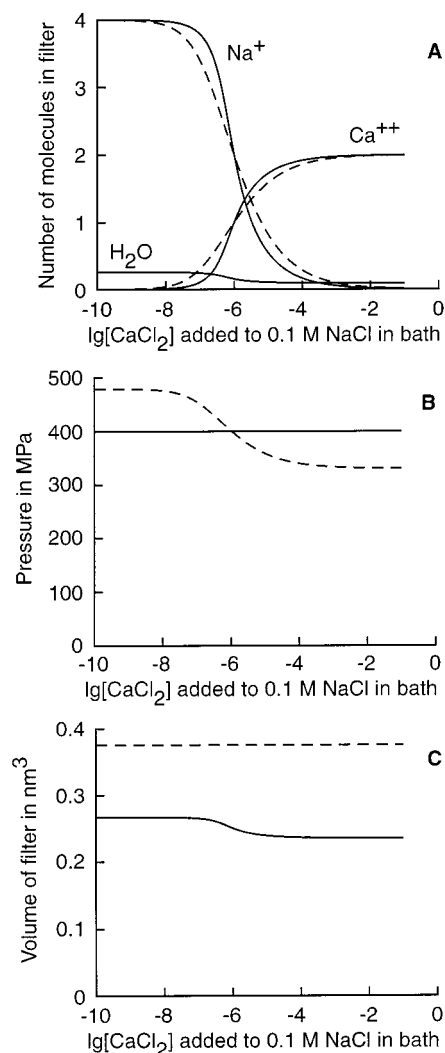
Figure 4. Comparison of the M2 (solid lines) and M1 models (dashed lines). (A) The number of ions and water (note that M1 uses the primitive model of water, so there are no water molecules). (B) The total pressure in the filter; this pressure is fixed by the protein in M2 but varies in M1. (C) The volume of the filter; the volume is fixed at 0.375 nm^3 in M1 but is variable in M2.

coefficient. Once in the filter, their mutual interactions are attenuated (i.e., screened) by the polarization described by the dielectric coefficient in the filter. The change in solvation energy between filter and bath is estimated by scaling experimental values of hydration energy according to the change in dielectric coefficient (eq 9). The attenuation of ion−ion interaction is directly described by the dielectric coefficient.

Computations presented thus far have been done with a fixed dielectric coefficient of 10 in the filter. If the dielectric coefficient is set to 20, physiological selectivity as described above can occur in the model, but only in a volume of $\approx$0.22 nm^3 with a confining pressure >1000 MPa, which seems unrealistic. On the other hand, if the dielectric coefficient is set to 5, the pressure in the filter is negative at the volume ($\approx$0.43 nm^3) where equivalent amounts of Ca^{2+} and Na^+ are accumulated into the filter. If the volume of the filter is then allowed to shrink until the pressure is, for example, 10^5 Pa, the final volume is $\approx$0.24 nm^3 and virtually all Na^+ is displaced by Ca^{2+} in the filter. If one postulates that the filter cannot collapse to volumes smaller than some limit (e.g., due to crowding among atoms of the filter wall), appropriate Ca^{2+}/Na^+ selectivity can occur even with a dielectric coefficient of

5. At bath concentrations of Ca^{2+} greater than 10 mM, however, the filter would accumulate Ca^{2+} *and* Cl^-, which contrasts with experiments that show conduction of Ca^{2+} but not Cl^- under such ionic conditions.[34] Together, these computations suggest that a dielectric coefficient around 10 results in adequate selectivity in this model of the EEEE locus, using the ion diameters listed in Table 1. (The choice of the ionic diameters is discussed below.)

A dielectric coefficient of $\approx$10 seems to be somewhat large given the small amounts of water that we find in the selectivity filter.[36] It seems possible that, in addition to the half-charged oxygens of the glutamate residues, the filter contains tethered hydroxyl or carbonyl oxygens. This has been observed in many Ca^{2+} binding proteins[37] and may be inferred from the sequence of the channel by considering the amino acids neighboring the four glutamates.[38] These polar oxygens could provide the induced charge described by the postulated dielectric coefficient.

We have done computations in which the filter contained several uncharged confined particles the size of oxygen. For instance, with four such particles included, physiological Ca^{2+}/Na^+ selectivity is seen if the volume and dielectric coefficient of the filter are $\approx$0.355 nm^3 and 7.4. Although such computations suggest that physiological selectivity is compatible with the "dilution" of charged oxygen ions by tethered (more or less) polar groups, an explicit description of ion−dipole and dipole−dipole interactions is needed. In this paper, we restrict analysis to a filter containing the carboxylate oxygens, but no inert or polar groups.

Ionic Diameters. Since the dielectric of the filter is weak, the change in solvation energy is large, >50 kT for Ca^{2+} (see the legend of Figure 3). This change of solvation energy must be closely balanced by ion−ion interactions (i.e., the sum of the electrostatic and excluded-volume energies) in the filter, if the model is to produce the small differences in chemical potential that underlie selectivity (see $\Delta\mu$ in Figure 3A). In general, these ion−ion interactions in the filter are sensitive functions of ionic diameter.

Shannon and Prewitt[39] tabulate crystal diameters based on metal−O^{2-} distances. These values depend on the properties of the oxygen and vary depending on how many oxygens are coordinated with the metal ion. Values corresponding to the coordination number 6 were used in NCE. In the present paper, we use ion diameters that depend on varying coordination numbers (see Table 1). This selection was guided by best fit to published experimental observations. The coordination numbers start from 5 for the small alkali ions, increase to 6 for the large alkali ions and anions, and go to 7 and 8 for divalent cations. This seems reasonable if one considers the valence of these ions and their usual coordination in salt crystals or in Ca-binding proteins that have been studied by X-ray diffraction.[37] Only Mg^{2+} breaks the general rule (among alkali and alkali earth ions) that, for a given valence, coordination number increases with atomic number. The Mg^{2+} diameter chosen here corresponds to a coordination number 8, which implies that the difference in Ca^{2+} and Mg^{2+} diameters is smaller than it would be if both ions had the same coordination number. The diameter needed for Mg^{2+} might, for example, describe a sterically restricted coordination between the oxygen ions of carboxylate groups and a very small divalent cation.

3.2. Ion Binding in the EEEE Locus. In this section, we present a specific model ("M2" for short) of the EEEE locus and discuss the selective ion binding in this model. We will refer to the PM-based, fixed-volume model proposed by NCE[10] as "M1".
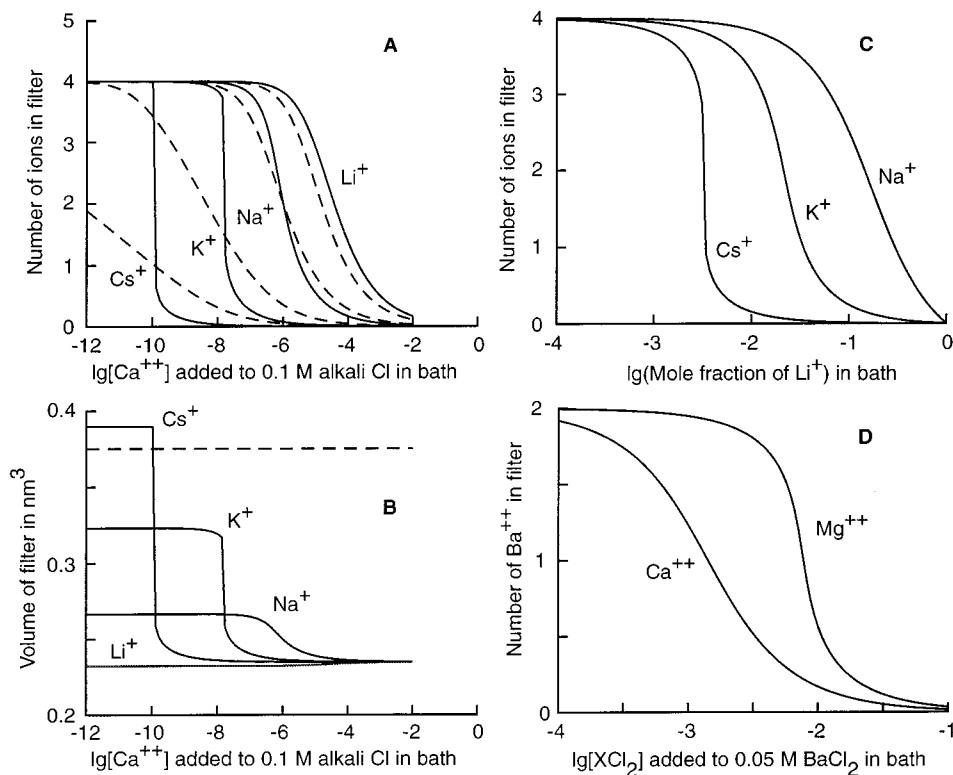
Figure 5. (A) Competition of alkali ions against Ca^{2+}; the ordinate plots the number of monovalent cations present in the filter; the bath contains 0.1 M of the chloride salt of the tested alkali cation and $CaCl_2$ is added as indicated on the abscissa. (B) The filter volumes corresponding to the simulations in panel A. (C) Competition of Li^+ against other alkali cations; the ordinate plots the number of test alkali ions in the filter; the bath contains the chloride salts of the test ion and Li at a fixed total concentration of 0.1 M, with the logarithm of the mole fraction of Li^+ shown on the abscissa. (D) Competition of Ba^{2+} against Ca^{2+} or Mg^{2+}; the ordinate gives the number of Ba^{2+} ions present in the filter when varied amounts of $CaCl_2$ or $MgCl_2$ are added to a 0.05 M $BaCl_2$ solution in the bath. Solid lines refer to M2, dashed lines to M1.

The M2 model assumes a constant confining pressure of 400 MPa, which is approximately the median pressure that occurs in the fixed volume of M1 (see Figure 4B). As in M1, the dielectric coefficient 10.5 was chosen so that Ca^{2+} is accumulated with the appropriate affinity over Na^+ (what we have called physiological selectivity).

The isotherms in Figure 4A give the computed numbers of Na^+ and Ca^{2+} ions (and water molecules for M2) that accumulate in the EEEE locus of the two models as the Ca^{2+} concentration is varied by adding $CaCl_2$ to a bath containing 0.1 M NaCl. Solid lines refer to M2, and dashed lines show M1 results for comparison. The situation corresponds to the experiments of refs 40−43. These experiments showed that, in L-type Ca channels, a large conductance supported by Na^+ is reduced to a smaller conductance supported by Ca^{2+} as Ca^{2+} is added in the bath. Half of this reduction of conductance is observed at about 1 μM Ca^{2+}. In kinetic descriptions of conduction, this reduction has been interpreted to mean that Ca^{2+} "blocks" the pore half of the time.[42,43] Here we interpret it to mean that the EEEE locus contains equivalent amounts of Na^+ and Ca^{2+}.[10]

Although both M1 and M2 predict accumulation of Ca^{2+} by the Ca channel, the models differ in other respects: (1) the volume of the EEEE locus described by M2 (under the protein pressure of 400 MPa) is only $\approx$2/3 the volume that generated comparable pressures in M1 (Figure 4C) and is due to the different models of water, as already discussed; (2) the isotherms predicted by M2 vary more steeply with bath composition than those of M1. The steeper isotherms are a consequence of the filter volume variation that occurs in M2, but not M1 (Figure 4C). This variation is accompanied by substantial variation of excess chemical potentials for the ions in the filter (cf. Figure

3A). If confining pressures smaller than 400 MPa are assumed in M2, the steepness of binding isotherms increases. With sufficiently small pressures (<100 MPa), Na^+/Ca^{2+} isotherms with stepwise transitions are computed. Then pressure/volume isotherms reveal a region of instability with a negative compressibility. The experimental data seem incompatible with Na^+/Ca^{2+} binding isotherms that include stepwise transitions. This suggests that the Ca channel protein confines the EEEE locus at effective pressures larger than 100 MPa.

Figure 5A shows binding isotherms computed for different alkali ions. As in Figure 4A, alkali ion concentration was maintained at 0.1 M in the bath while $CaCl_2$ was added to the bath as shown on the abscissa. In all simulations the M2 parameters (400 MPa of confining pressure and filter dielectric coefficient of 10.5) were unchanged. The two models (M1, dashed lines; M2, solid lines) give substantially different predictions for the accumulation of large alkali ions. The M1 binding curves are continuous and their slopes decrease as ion diameters increase. This is because the excluded volume of large ions counteracts their accumulation in the fixed filter volume of M1. This effect is so strong that, even at 10^{-10} M Ca^{2+} in the bath, neither K^+ nor Cs^+ can neutralize the four negative charges in the filter by itself. In M2, on the other hand, the larger excluded volume pressures can be relieved by increasing the filter volume (Figure 5B), which in turn weakens the ion/ion interactions inside the filter (cf. Figure 3A) and thus the electrostatic cohesive pressure (cf. Figure 2B). Because of this internal feedback, the M2 isotherms steepen as the monovalent ion diameters increase. The K^+ and Cs^+ isotherms even have a discontinuity that allows the M2 filter to accept electrostatically saturating amounts of K^+ and Cs^+ where the M1 filter could not.

Ion Accumulation in a Biological Ca Channel

J. Phys. Chem. B, Vol. 105, No. 27, 2001 **6435**

We are not aware of published experimental data describing the competition between Cs^+/Ca^{2+} or K^+/Ca^{2+} that could be used to compare with the curves in Figure 5A. Experiments using the protocol of Almers and McCleskey,[42] which tests the competition between Ca^{2+} and an alkali species, could examine whether Cs^+ or K^+ binding reveal the signature of variable volume in the EEEE locus, namely steepening of the isotherms with increasing diameter of the tested monovalent cation. This protocol, however, requires accurate buffering of very small Ca^{2+} concentrations in bath solutions, which might be compromised by the dependence of available Ca buffers on alkali metal ions. Such buffers involve a cluster of tethered carboxylate groups such as the EEEE locus, and so their Ca^{2+} buffering might depend sensitively on the species of monovalent ions in the bath (cf. Figure 5A).

One way to overcome this difficulty in Ca^{2+} buffering is to work with divalent-free solutions, for example, by varying the mole fraction of Na^+, K^+, or Cs^+ with a complement of Li^+. Figure 5C shows simulations of such an experiment, where the abscissa gives the logarithm of the mole fraction of Li^+. As in Figure 5A, the slopes of these isotherms in Figure 5C also increase from Na^+ to Cs^+.

On the other hand, in experiments with only divalent cations, when varying amounts of added Ca^{2+} or Mg^{2+} compete with 50 mM Ba^{2+}, half the Ba^{2+} in the filter appears to be displaced at bath concentrations of a few millimolar Ca^{2+} or ≈ 10 mM Mg^{2+}.[44] These observations are well-reproduced by M2 using the ion diameters of Table 1 (Figure 5D). M1 also described the Ba^{2+}/Ca^{2+} competition data, but to describe the Mg^{2+}/Ca^{2+} data, it required a larger diameter for Mg^{2+} than for Ca^{2+}.[10] The M2 results were obtained by assigning Mg^{2+} a diameter that is substantially smaller than the diameter used for Ca^{2+}, but the Mg^{2+} diameter that best reproduced the data corresponded to a larger coordination number than for Ca^{2+} (8 compared to 7; see Table 1).

It thus seems that M2 eliminates the Mg^{2+} "anomaly" that was previously found with M1. The relevant difference between the two descriptions of ion accumulation in this case is their treatment of solvation. In M2 we use experimental bulk hydration energies that are specific for each ion and estimate the solvation energies in the filter by scaling bulk hydration energies in inverse proportion to the dielectric coefficient in the filter (eq 9). The hydration energy for Mg^{2+} is very large, and hence, the change in solvation energy in going from the bath to the filter is particularly unfavorable for this ion. This is evident in Figure 3A, where $\Delta\mu_{Mg}$ is substantially more positive at large filter volumes than for any other ion. The ionic interactions in the filter, which underlie the excess chemical potentials of eq 24, do not compensate for the unfavorable solvation energy of Mg^{2+} to the same extent they do for Ca^{2+}. The inclusion of hydration in M2 then eliminates the unsatisfactory possibility suggested by M1 that Mg^{2+} has particularly weak ion–ion interactions inside the filter.

3.3. The EEEE Locus Viewed as Transducer of a Ca^{2+} Signal. Our model of Ca^{2+} accumulation in L-type Ca channels makes no reference to the specific channel shape or structure, only to the presence of oxygen ions inside the channel. Many proteins that are regulated by variations of intracellular Ca^{2+} concentration[45–47] have Ca binding sites with oxygen ions from glutamate or aspartate residues and formally uncharged oxygen atoms of the protein. The similarity between the EEEE locus and regulatory Ca^{2+} binding sites suggests that the M2 model might be usefully applied to model the binding of calcium to the protein and to determine the consequences of that binding.
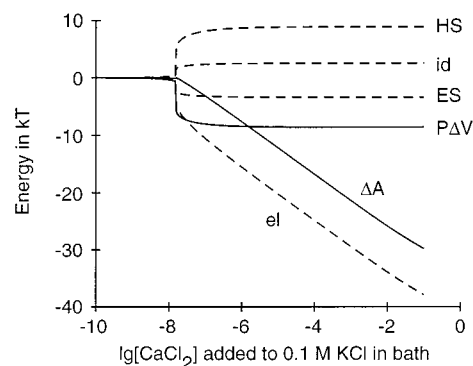
Figure 6. Energetics of K^+/Ca^{2+} exchange. All energies shown are relative to those obtained with pure 0.1 M KCl in the bath. $P\Delta V$ is the volume work done on the protein. ΔA is the change in availability (eq 8), which equals the change in Gibbs energy experienced by the oxygen ions and can be expressed in the components: el, the electric energy of the oxygens due to the Donnan potential; id, the (ideal) concentration work due to the change in filter volume; ES, the excess energy of the electrostatic oxygen–ion interaction, which varies directly with ionic density; HS, the excess energy due to the excluded-volume interactions in the filter, which also varies directly with ionic density.

One link between the protein and the binding is the electric field that emanates from the binding site;[10] the electric field will vary as the concentration of Ca^{2+} in the bath and the occupancy of the binding site change. On the other hand, the link between the protein and the occupancy of the binding site might also be mechanical: a site described by the M2 model, with a variable locus volume, *automatically* involves mechanical forces and movement.

How much does Ca^{2+} concentration have to change to make mechanical work available? How much mechanical work can be exchanged between the binding site and a regulated protein with a high sensitivity for Ca^{2+}? Figure 6 plots the energetics when K^+ is replaced by Ca^{2+} in the M2 model of the EEEE locus. We choose K^+ because it is the most abundant alkali cation inside cells, where most Ca-regulated proteins reside. All energies shown are referenced to the energies computed with a pure KCl bath. The curves give the availability (ΔA) [which can be expressed as the Gibbs energy of the oxygen ions (eq 8)], and its components are represented by the ideal (id), electrical (el), excess electrostatic (ES), and hard-sphere (HS) contributions. The volume work done (eq 1) is shown as the curve labeled $P\Delta V$.

It is clear that substantial volume work (7–8 kT) can be derived from this system when Ca^{2+} is added to a 0.1 M KCl bath. (If the monovalent cation were Na^+, which is smaller than K^+, only about half that work would be available.) Furthermore, this volume work becomes available over a very narrow range of Ca^{2+} concentration in the bath when concentrations are low, just the properties needed to make a Ca^{2+} binding site function as an effective molecular switch.

Under these conditions, the volume of the selectivity filter jumps when four K^+ exchange for two Ca^{2+}. The volume work done involves substantial rearrangements in the components of the Gibbs energy of the oxygen ions even though the total Gibbs energy of the oxygens is almost unchanged. It is mainly the changes in excluded volume and electrical potential that are immediately translated into a change of site volume, flipping the switch. As the Ca^{2+} concentration is increased beyond the threshold needed for the switch, the Gibbs energy changes substantially, but this does not result in much further volume work that can be exploited by the protein.

The Ca^{2+} regulatory site acts as a mechanical switch for two reasons in this model. First, there is essentially no water in the

binding site that could be displaced by large ions; instead, the excluded-volume effects of the K^+ force an expansion of the site. Indeed, X-ray diffraction has shown that at most one water oxygen participates in the coordination of the Ca^{2+} in such proteins.[48] Second, the protein maintains a positive confining pressure on the site. Mechanical work is done on the protein when Ca^{2+} *leaves* the site and is replaced by monovalent cations. If the site were constructed so that entry of Ca^{2+} into the site generated a swelling (negative) pressure, particles from the bath could fill the void in the site. Little mechanical work would be done on the protein itself and the protein would not act as a mechanical switch.

Conclusion

Our computations suggest that structural oxygen ions and mobile ions accumulated in the EEEE locus of Ca channels form a dense ionic cluster that virtually excludes water with the dehydration of accumulated ions energetically compensated by strong interionic interactions. Selectivity based on excluded volume occurs if the protein confines the locus at pressures that ensure a packing fraction larger than that in the bath. Physiological selectivity is found if electrostatics in the filter is moderated by a local dielectric coefficient of ≈ 10. Furthermore, the modeled EEEE locus can accommodate relatively large ions if the confinement by the protein allows for some volume expansion. Such volume changes of the locus make ion accumulation in the locus more steeply dependent on the composition of a mixed bath. We showed that substantial volume work can be done on the protein when Ca^{2+} is replaced by K^+ in such a locus.

References and Notes

(1) Rasmussen, H.; Barrett, P. Q. *Physiol. Rev.* **1984**, *64*, 938.
(2) Heinemann, S. H.; Terlau, H.; Stühmer, W.; Imoto, K.; Numa, S. *Nature* **1992**, *356*, 441.
(3) Kim, M. S.; Morii, T.; Sun, L.-X.; Imoto, K.; Mori, Y. *FEBS Lett.* **1993**, *318*, 145.
(4) Mikala, G. A.; Bahinski, A.; Yatano, A.; Tang, S.; Schwartz, A. *FEBS Lett.* **1993**, *335*, 265.
(5) Tang, S.; Mikala, G.; Bahinski, A.; Yatani, A.; Varadi, G.; Schwartz, A. *J. Biol. Chem.* **1993**, *268*, 13026.
(6) Yang, J.; Ellinor, P. T.; Sather, W. A.; Zhang, J.-F.; Tsien, R. W. *Nature* **1993**, *366*, 158.
(7) Yatani, A.; Bahinski, A.; Mikala, G.; Yamamoto, S.; Schwartz, A. *Circ. Res.* **1994**, *75*, 315.
(8) Parent, L.; Gopalakrishnan, M. *Biophys. J.* **1995**, *69*, 1801.
(9) Cibulsky, S. M.; Sather, W. A. *J. Gen. Physiol.* **2000**, *116*, 349.
(10) Nonner, W.; Catacuzzeno, L.; Eisenberg, B. *Biophys. J.* **2000**, *79*, 1976.
(11) Boda, D.; Busath, D. D.; Henderson, D.; Sokołowski, S. *J. Phys. Chem. B* **2000**, *104*, 8903.
(12) Boda, D.; Henderson, D.; Busath, D. D. *J. Phys.Chem. B* In press.
(13) Henderson, D.; Lozada-Cassou, M. *J. Colloid Interface Sci.* **1986**, *114*, 180.
(14) Davis, H. T.; Zhang, L.; White, H. S. *J. Chem. Phys.* **1993**, *98*, 5793.
(15) Boda, D.; Henderson, D. *J. Chem. Phys.* **2000**, *112*, 8934.
(16) Goulding, D.; Melchionna, S.; Hansen, J.-P. *Phys. Rev. Lett.* **2000**, *85*, 1132.
(17) Goulding, D.; Melchionna, S.; Hansen, J.-P. *Phys. Chem. Chem. Phys.* Submitted.
(18) Moy, V.; Florin, E. L.; Gaub, H. E. *Science* **1994**, *266*, 257.
(19) Oesterhelt, F.; Oesterhelt, D.; Pfeiffer, A.; Engel, A.; Gaub, H. E.; Müller, D. J. *Science* **2000**, *288*, 143.
(20) Nonner, W.; Eisenberg, B. *Biophys. J.* **1998**, *75*, 1287.
(21) Mandl, F. *Statistical Physics*; John Wiley and Sons: Chichester, UK, 1988.
(22) Waisman, E.; Lebowitz, J. L. *J. Chem. Phys.* **1972**, *56*, 3093.
(23) Blum, L. *Mol. Phys.* **1975**, *30*, 1529.
(24) Triolo, R.; Grigera, J. R.; Blum, L. *J. Phys. Chem.* **1976**, *80*, 1858.
(25) Triolo, R.; Blum, L.; Floriano, M. A. *J. Phys. Chem.* **1978**, *82*, 1368.
(26) Triolo, R.; Blum, L.; Floriano, M. A. *J. Chem. Phys.* **1978**, *67*, 5956.
(27) Blum, L.; Hoye, J. S. *J. Phys. Chem.* **1977**, *81*, 1311.
(28) Simonin, J.-P.; Blum, L.; Turq, P. *J. Phys. Chem. B* **1996**, *100*, 7704.
(29) Simonin, J.-P. *J. Phys. Chem. B* **1997**, *101*, 4313.
(30) Born, M. Z. *Phys.* **1920**, *1*, 45.
(31) Lebowitz, J. L. *Phys. Rev.* **1964**, *133*, A895.
(32) Salacuse, J. J.; Stell, G. *J. Chem. Phys.* **1982**, *77*, 3714.
(33) Press, W. H.; Teukolsky, S. A.; Vetterling, W. T.; Flannery, B. P. *Numerical Recipes in C*, 2nd ed.; Cambridge University Press: Cambridge, UK, 1992.
(34) Hess, P.; Lansman, J. B.; Tsien, R. W. *J. Gen. Physiol.* **1986**, *88*, 293.
(35) McCleskey, E. W.; Almers, W. *Proc. Natl. Acad. Sci. U.S.A.* **1985**, *82*, 7149.
(36) Blum, L.; Vericat, F.; Fawcett, W. R. *J. Chem. Phys.* **1992**, *96*, 3039.
(37) Nelson, M.; Chazin, W. *Biometals* **1998**, *11*, 297.
(38) Narahashi, T. *Ion Channels*; Plenum Press: NewYork, 1996.
(39) Shannon, R. D.; Prewitt, C. T. *Acta Crystallogr. B* **1969**, *25*, 925.
(40) Kostyuk, P. G.; Mironov, S. L.; Shuba, Y. M. *J. Membr. Biol.* **1983**, *76*, 83.
(41) Almers, W.; McCleskey, E. W.; Palade, P. T. *J. Physiol.* **1984**, *353*, 565.
(42) Almers, W.; McCleskey, E. W. *J. Physiol.* **1984**, *353*, 585.
(43) Hess, P.; Tsien, R. W. *Nature* **1984**, *309*, 453.
(44) Lansman, J. B.; Hess, P.; Tsien, R. W. *J. Gen. Physiol.* **1986**, *88*, 321.
(45) Clapham, D. E. *Cell* **1995**, *80*, 259.
(46) Ikura, M. *Trends Biochem. Sci.* **1996**, *21*, 14.
(47) Bootman, M. D.; Berridge, M. J. *Cell* **1995**, *83*, 675.
(48) Drake, S. K.; Zimmer, M. A.; Kundrot, C.; Falke, J. J. *J. Gen. Physiol.* **1997**, *110*, 173.
(49) Fawcett, W. R. *J. Phys. Chem. B* **1999**, *103*, 11181.